

NASA Technical Paper 1039

Laboratory Measurements of Upwelled Radiance and Reflectance Spectra of Calvert, Ball, Jordan, and Feldspar Soil Sediments

Charles H. Whitlock, J. W. Usry,
William G. Witte, and E. A. Gurganus
Langley Research Center
Hampton, Virginia



National Aeronautics
and Space Administration

**Scientific and Technical
Information Office**

1977

SUMMARY

A limited effort to investigate the potential of remote sensing for monitoring non-point source pollution was conducted. Spectral reflectance characteristics for four types of soil sediments were measured for mixture concentrations between 4 and 173 ppm. For measurements at a spectral resolution of 32 nm, the spectral reflectances of Calvert, Ball, Jordan, and Feldspar soil sediments were distinctly different over the wavelength range from 400 to 980 nm at each concentration tested. At high concentrations, spectral differences between the various sediments could be detected by measurements with a spectral resolution of 160 nm. At a low concentration (4 ppm), only small differences were observed between the various sediments when measurements were made with 160-nm spectral resolution. Radiance levels generally varied in a nonlinear manner with sediment concentration; linearity occurred in special cases, depending on sediment type, concentration range, and wavelength.

INTRODUCTION

The 1983 water quality goals listed in Public Law 92-500 will not be attainable without control of nonpoint source (NPS) pollution. (See refs. 1 and 2.) NPS categories contributing substantially to pollution are, for example, urban runoff, rural runoff, construction activities, and hydrologic modification. NPS pollutants of greatest concern are sediments, pesticides, toxic metals, nutrients, pathogens, BOD (biochemical oxygen demand), dissolved solids, coarse and floatable solids, and toxic organic compounds. As a result of the broad expanse of NPS discharge, it is often difficult for an observer to identify the pollutant source precisely. It is believed that remote sensing techniques with wide-area, synoptic coverage may aid in the detection and location of NPS pollutant sources enabling the design of more effective control systems on the ground (dikes, culverts, etc.). Recent Environmental Protection Agency (EPA) field studies have shown that 98 percent of all water pollution sources are detectable by changes in color or temperature which may be monitored with remote sensing instrumentation (ref. 3).

Much has been published (refs. 4 to 7, for example) concerning the ability of remote sensing to monitor water circulation patterns and water quality parameters. The problem with remote sensing of NPS pollution is the present lack of knowledge of how various pollutant constituents influence the radiance at various wavelengths (known as a spectral signature) which is upwelled through the water surface. It is unknown whether various

types of soil sediments have different spectral signatures and whether certain pollutants either have their own spectral signatures or perhaps modify that of the sediment through chemical sorption processes. A knowledge of spectral signature characteristics of basic soil sediments is needed before remote sensing techniques can be used reliably to aid monitoring of NPS pollution. Only with such fundamental knowledge can procedures be developed for relating changes in remotely sensed upwelled radiance to variations in sediment concentration or to detection of new constituents entering the water.

In cooperation with the EPA and other federal agencies, the National Aeronautics and Space Administration is conducting an extensive research program to evaluate the feasibility of remote sensing of environmental quality parameters in water. One aspect of the overall research program is laboratory measurement of upwelled spectral signatures from water for various soil sediments. In the final analysis, tests of actual sediments from water bodies at various geographical locations will be required to assess fully the potential of remote sensing for monitoring NPS pollution. To provide fundamental information in preparation for such activities, it was decided to test a series of different soil types which could be obtained in controlled batches. Calvert, Ball, Jordan, and Feldspar soils were selected for these tests because (1) they are obtainable from controlled mines in a near-pure state, (2) they are different in color at visible wavelengths, (3) they have different particle size distributions, (4) they have different mineral content, and (5) they are typical of materials which make up the soil sediments at many locations in the eastern United States. Calvert soil is red in color, and Ball soil is a gray clay. Jordan soil is a gray-red color, and Feldspar is almost pure white. Mineral content and particle size distribution for these soils are given in reference 8. Spectral variations in transmission and attenuation coefficient are given in reference 9 for these soils. It is the purpose of this document to present laboratory-measured upwelled spectral signature characteristics of the Calvert, Ball, Jordan, and Feldspar soil sediments. Specifically, upwelled spectral radiance and reflectance characteristics are presented, and the relation between reflectance and concentration (whether nonlinear or linear) is examined at several wavelengths for each sediment type.

SYMBOLS

| | |
|--------------|---|
| A | area of spectrometer entrance slit, cm^2 |
| D | vertical displacement of oscilloscope measurement, cm |
| $E(\lambda)$ | spectral irradiance, $\text{W}/\text{m}^2\text{-nm}$ |

| | |
|-------------------|--|
| K | ratio of instrument throughput $A\Omega$ to vertical-scale sensitivity factor S , $\text{cm}^3\text{-sr-nm/mW}$ |
| $L_u(\lambda)$ | upwelled spectral radiance, $\text{mW/cm}^2\text{-sr-nm}$ |
| $P(\lambda)$ | spectral power, mW/nm |
| S | vertical-scale sensitivity factor, mW/cm-nm |
| λ | wavelength, nm |
| $\rho_u(\lambda)$ | spectral reflectance (relative to a 100-percent diffuse reflector), percent of input |
| σ | standard deviation of instrument error |
| Ω | acceptance solid angle of spectrometer, sr |

LABORATORY AND EQUIPMENT

Figure 1 is a sketch of the laboratory arrangement. Major parts of the setup include a water tank, circulation system, filtration and deionization system, solar simulator, first-surface mirror, and rapid-scan spectrometer. A black canvas tent covers the water tank to block out background radiation during testing and to prevent contamination of the water tank (by dust, for example).

The cylindrical steel water tank has a 2.5-m diameter and a 3-m depth. The bottom is concave as illustrated in figure 1. The tank interior is coated with a black phenolic paint that absorbs 97 percent of incident radiation over the spectral range of these measurements (400 to 980 nm). For these experiments, the tank was filled to within 0.3 m of the top with about 11 600 liters of water.

The circulation system was designed to maintain a vertical and horizontal homogeneous mixture in the tank and to maintain in suspension particles up to about $100\ \mu\text{m}$ in diameter (specific gravity of 2.6). This particle size corresponds to fine sand. To accomplish these design goals, water is pumped from the drain at the bottom of the tank into a system of pipes which returns the water to the tank through two vertical pipes on opposite sides of the tank. The pipes empty just above the concave bottom. Water entering the tank through these pipes washes over the concave bottom, meets at a location away from the drain, and wells upward. Tests using tracer techniques and transmission

measurements have confirmed that this circulation system provides a near-uniform homogeneous mixture throughout the tank. For pollutants such as sewage sludge with specific gravities less than 2.6, the present laboratory setup can suspend particles larger than 100 μm in diameter.

The filtration and deionization system includes a commercial fiber swimming-pool filter, an activated carbon filter, and a charged resin deionizer. These units were placed in water lines parallel to the main circulation system water lines and can be used separately or in any combination by using valves. The two filters remove inorganic and organic particulates from the water before it reaches the deionizer where dissolved ionic substances are removed. After tap water is conditioned through this system, it contains less than 0.5 ppm of suspended solids and less than 2 ppm of dissolved substances.

The light source is a solar-radiation simulator designed to approximate the spectral content of the Sun's rays. The radiation spectrum is produced by a 2.5-kW xenon short-arc lamp and transferred to the target plane through an optical arrangement inside the simulator and a collimating lens accessory. With the collimating lens accessory, the projected beam is collimated to a 0.15-m diameter, 0.3 m from the simulator and has a $\pm 2.5^\circ$ collimation angle. For these experiments, the simulator was located approximately 15.2 m from the water tank as illustrated in figure 1. At this distance from the simulator, the beam is about 1.2 m in diameter. A mirror positioned 1.52 m above the water tank reflects the center of the beam to the water surface. The incidence angle with the water surface is 13° to avoid specular reflectance. The mirror is a first-surface mirror coated with aluminum and protected by an overcoat of silicon monoxide. It has a 0.3-m diameter and reflects an elliptical spot on the water surface which has a maximum diameter of 0.35 m. The simulator spectral input to the water surface is similar to, but not a precise duplicate of, sea-level standard solar-radiation curves often used in engineering calculations (ref. 10). Figure 2(a) shows that the standard sea-level curves are quite variable depending on the solar elevation angle. Figure 2(b) is the simulator spectrum normalized at 600 nm to the solar spectrum at a solar elevation angle of 30° . These curves suggest that when laboratory measurements are made at a 32-nm spectral resolution, the input spectrum and possibly the output measurements are similar to those that would be expected in the field if the solar elevation angle is on the order of 30° . The total intensity of the light hitting the water surface is approximately 8 percent of that in actual field conditions.

The rapid-scanning spectrometer system consists of a spectrometer unit with a telephoto lens attachment and a plug-in unit with an oscilloscope and Polaroid camera attachment. The spectrometer unit with telephoto lens attachment is mounted 2.43 m above the surface of the water as illustrated in figure 1. The spectrometer uses a Czerny-Turner grating monochromator without an exit slit. The spectral output of the

monochromator is focused on the target of a vidicon tube where the spectrum is stored as an electrical charge image. An electron beam periodically scans the vidicon target to convert the charge image into an electronic signal. This signal is processed by the plug-in unit which functions as an electronic signal processor and controller between the spectrometer and the oscilloscope. The signal is displayed on the oscilloscope and is photographically recorded with the camera. The spectrometer is designed to measure power per spectral bandwidth (spectral power). The oscilloscope screen is used to show displacement of the instrument measurement. Oscilloscope displacement is proportional to spectral power, as shown in the following equation:

$$D = \frac{P(\lambda)}{S} \quad (1)$$

The signal is internally processed in such a manner that the vertical-scale sensitivity factor S has a constant value over the wavelength range from 400 to 980 nm. Values of S were obtained by the manufacturer using calibration procedures described in reference 11. (After receipt of the instrument, the manufacturer's calibration was checked in an approximate manner prior to the tests described herein.) The upwelled spectral radiance $L_u(\lambda)$ is defined as

$$L_u(\lambda) = \frac{P(\lambda)}{A\Omega} \quad (2)$$

where A is the area of the spectrometer entrance slit and Ω is the acceptance solid angle of the spectrometer. Radiance values given in this document are based on power received at the detector and are not corrected for losses through the telephoto lens. Tests with and without the lens indicate that such losses are much less than 5 percent for wavelengths between 400 and 980 nm.

Combining equations (1) and (2) results in

$$L_u(\lambda) = \frac{DS}{A\Omega} \quad (3)$$

or

$$L_u(\lambda) = \frac{D}{K} \quad (4)$$

where

$$K = \frac{A\Omega}{S}$$

Thus, upwelled spectral radiance is determined from oscilloscope displacement and the proportionality constant K which is a function of the calibration factor S (which includes optical transmissivity) as well as acceptance angle Ω and slit area A .

The instrument has been observed to experience daily variations in the calibration factor K which affect absolute accuracy. According to instrument specifications, absolute accuracy of the measurements is believed to be ± 20 percent in the 400- to 600-nm range and ± 12 percent in the 600- to 900-nm range. (Comparison of results from a number of laboratory tests at NASA tends to verify the manufacturer's specifications.) Included in the absolute error is a repeatability uncertainty of ± 13 percent in the 400- to 600-nm range and ± 3.5 percent in the 600- to 900-nm range. Discussions with the manufacturer indicate that these values are believed to be representative of 3σ error bands. Because of these absolute errors, spectral radiances from tests conducted on different days usually differ somewhat in magnitude. The overall shape of the spectra over the wavelength range is quite consistent between tests conducted on different days, however.

By adjusting the slit area, spectral resolution of the spectrometer may be changed. For the tests described herein, repetitive measurements were made at two different spectral resolutions to assess the effect of spectral bandwidth on observing differences between the four sediment types. Spectral resolutions of 32 nm and 160 nm were selected for the laboratory tests. The 160-nm resolution was the widest bandwidth available on the spectrometer. Because of the low intensity of the light source, acceptable signal-to-noise performance was not achieved for measurements at spectral resolutions less than 32 nm. Data at spectral resolutions of 32 nm and 160 nm are applicable because several aircraft and satellite multispectral scanners have bandwidths within this range.

EXPERIMENTAL METHOD

A series of eight experiments was conducted over a 6-month period to obtain upwelled radiance spectra for each soil type. The soil materials were obtained in a dry state from controlled mines. Mined materials which met certain ceramic specifications were selected for use so that large quantities of near-similar material would be available for repetitive testing. The materials were further tested (ref. 8) to confirm their adherence to suppliers' specifications as to size distribution and mineral content.

Each experiment was conducted by first filling the tank with approximately 11 600 liters of conditioned (filtered and deionized) tap water. Measured weights of dry soil were then mixed with the tank water in succession to achieve increasing levels of sediment concentration. Spectral measurements were generally made at mixture concentrations of 4, 17, 35, 69, 86, 129, and 173 ppm by weight. The conditioned tap water to

which the sediments were added contained less than 0.5 ppm of suspended solids and 2 ppm of dissolved substances.

For each concentration level, the circulation system was activated (bypassing the filter-deionization system). Radiance measurements could not begin until a steady-state condition with near-uniform sediment concentration was achieved. Tests were conducted with a submerged transmissometer, and it was found that approximately 15 minutes of mixing was required for transmission readings to become both stable and near uniform at all locations within the tank. On the basis of transmission readings, it is believed that the variation in concentration from spot to spot in the tank was less than 0.5 ppm. Considering inaccuracies in filling the tank, errors in successive weight measurements, and inconsistency in tap water, the absolute accuracy of each concentration value is believed to be 0.5 ppm or 5 percent of the quoted value, whichever is higher.

Generally, after the water tank was first filled, 3 to 4 hours were required to complete an experiment. Before, during, and after each experiment, diffuse reflectance measurements of the solar simulator input at the water surface were made to monitor optical stability of the laboratory system. In addition, these input light spectra were used to derive spectral reflectance from upwelled spectral radiance values for each sediment. Spectral reflectance is the upwelled spectral radiance of the water mixture divided by the diffuse reflectance (after correction to a 100-percent diffuse reflector) of the input light.

RESULTS AND DISCUSSION

Measured spectral radiance curves are shown in figures 3 to 6 for each soil type. Variations in the curves between 750 and 950 nm are caused by the spectral characteristics of the input xenon light source and are not believed to be related to the spectral response of the sediments. These variations are observed only in the narrow-band (spectral resolution of 32 nm) data because at wide spectral resolutions the peaks and valleys of the input xenon lamp spectra are averaged over the optical bandwidth (spectral resolution) of the spectrometer. The displacement value at any particular concentration and wavelength is an average over the spectral resolution. For example, values shown at 600 nm are an average of values from 584 to 616 nm for the narrow-band data. For the wide-band data, each point represents an average of values lying within 80 nm to each side of the wavelength of interest. Thus, the wide-band spectrum for each soil appears as a smoothed version of the narrow-band spectrum for the same soil. For each soil type, the wide-band and narrow-band tests were conducted on different days; hence, the magnitudes of spectral radiance values show some differences because of instrument variations, as previously discussed.

Spectral reflectance curves are shown in figures 7 to 10 for each soil type. For the wavelength region of the xenon spikes (750 to 980 nm), the curves shown in figures 7(a), 8(a), 9(a), and 10(a) were obtained by fairing between scattered spectral reflectance values. Scattered values were obtained because of the problem of making an accurate reading on steep slopes in the vicinity of sharp spikes. Little fairing was required for wavelengths below 750 nm. This problem was not experienced with the wide-band data.

Comparisons of spectra for the various soil sediments are shown in figure 11 for concentrations of 86 ppm. From this figure, it is concluded that each of the tested sediment types has a distinct spectral reflectance for both the wide- and narrow-band spectral resolutions when high mixture concentrations exist. At low concentrations, differences between the observed spectra are not as distinct, depending on spectral resolution. For a concentration of 4 ppm, significant differences between some of the sediments are detectable with a spectral resolution of 32 nm (fig. 12(a)). For a spectral resolution of 160 nm (fig. 12(b)), there are only slight spectral differences between the sediments. These results suggest that remote sensing instruments with narrow spectral resolution may be required for those environmental situations where low sediment concentrations exist, but wide-band systems (such as the Landsat satellites) may have application for monitoring nonpoint source pollution in waters where highly turbid conditions exist. Field experiments with the particular systems that have appropriate spacial resolution for the geographic area under investigation are required to confirm this hypothesis, however.

Under high concentration conditions (fig. 11(a)), there is a distinct spectral difference between red clay (Calvert) and gray clay (Ball). Also, the spectrum for white Feldspar is quite different. However, the spectrum of the gray-red clay (Jordan) is similar to that of Ball clay, and it is possible that there may be gray-red soil sediment types that are difficult to distinguish with remote sensing instrumentation in the visible and near-infrared regions. Since the Feldspar soil of these tests is somewhat similar (by its high quartz content) to some sands, figure 11(a) suggests that it may be possible to distinguish between sand and clay sediments with remote sensing instruments. However, additional laboratory tests with actual sand are required to evaluate this possibility. Such information on mineral content is desired by many user agencies (ref. 12).

The variation of spectral reflectance as a function of sediment concentration is shown in figure 13 for wavelengths of 500, 600, and 700 nm. Within the accuracy of these tests, both Feldspar and Jordan sediments appear to vary nearly linearly with concentration over the range tested (4 to 173 ppm). The Calvert and Ball sediments show definite nonlinearities at some wavelengths, however. From these data, it is concluded that some sediments have a nonlinear variation of spectral reflectance with concentration and the

degree of nonlinearity is a function of wavelength. It is not presently known whether the degree of linearity varies as the base water is changed. Additional tests are required to investigate the effects of base water on linearity characteristics. Such tests should be conducted in both filtered, deionized tap water (as in these tests) and in river water with dissolved substances and other particulates. The linearity of upwelled spectral radiance must be established if accurate data analysis procedures are to be developed for quantification of water quality parameters from remote sensing data.

CONCLUDING REMARKS

Spectral reflectance characteristics of Calvert, Ball, Jordan, and Feldspar soil sediments were measured for water mixture concentrations between 4 and 173 ppm. The results of these laboratory measurements indicate the following:

1. For a spectral resolution of 32 nm, the spectral reflectances of Calvert, Ball, Jordan, and Feldspar soil sediments are generally different over the concentration range from 4 to 173 ppm.
2. At high concentrations, spectral differences between the various sediments can be detected by measurements with a spectral resolution of 160 nm.
3. At a low concentration (4 ppm), only small differences are observed between the spectra of the various sediments when measurements were made with 160-nm spectral resolution.
4. Radiance levels generally varied in a nonlinear manner with water mixture concentration; linearity occurred in special cases, depending on sediment type, concentration range, and wavelength.

Additional laboratory tests are recommended which use actual marine sediments to evaluate the influence of different base waters on spectral reflectance characteristics. Little is known concerning the influence of other pollutants on the spectral signature of various sediments.

Langley Research Center
National Aeronautics and Space Administration
Hampton, VA 23665
November 17, 1977

REFERENCES

1. Environmental Quality. Fifth Annual Report of the Council on Environmental Quality, Dec. 1974.
2. Environmental Quality – 1976. Seventh Annual Report of the Council on Environmental Quality, Sept. 1976.
3. Melfi, S. H.; Koutsandreas, John D.; and Moran, John: Tracking Pollutants From a Distance. Environ. Sci. & Technol., vol. 11, no. 1, Jan. 1977, pp. 36-38.
4. Klemas, V.; Otley, M.; Philpot, W.; Wethe, C.; Rogers, R.; and Shah, N.: Correlation of Coastal Water Turbidity and Current Circulation With ERTS-1 and Skylab Imagery. Proceedings of the Ninth International Symposium on Remote Sensing of Environment, Volume II, Environ. Res. Inst. of Michigan, Apr. 1974, pp. 1289-1317.
5. Christensen, R. J.; and Wezernak, C. T.: Use of Remote Sensing for Water Resource Management in Michigan. Proceedings of Tenth International Symposium on Remote Sensing of Environment – Volume I, Environ. Res. Inst., Univ. Michigan, Oct. 1975, pp. 485-494.
6. Yarger, Harold L.; and McCauley, James R.: Quantitative Water Quality With LANDSAT and SKYLAB. NASA Earth Resources Survey Symposium. Volume 1-A: Technical Session Presentations – Agriculture, Environment, NASA TM X-58168, 1975, pp. 347-370.
7. Johnson, Robert W.; and Bahn, Gilbert S.: Quantitative Analysis of Aircraft Multi-spectral Scanner Data and Mapping of Water-Quality Parameters in the James River in Virginia. NASA TP-1021, 1977.
8. Chapman, Raymond S.: Particle Size and X-Ray Analysis of Feldspar, Calvert, Ball, and Jordan Soils. NASA TM X-73941, 1977.
9. Ghovanlou, A.: Radiative Transfer Model for Remote Sensing of Suspended Sediments in Water. NASA CR-145145, 1977.
10. Moon, Parry: Proposed Standard Solar-Radiation Curves for Engineering Use. J. Franklin Inst., vol. 230, no. 5, Nov. 1940, pp. 583-617.
11. Stair, Ralph; Johnston, Russell G.; and Halbach, E. W.: Standard of Spectral Radiance for the Region of 0.25 to 2.6 Microns. J. Res. Natl. Bur. Stand., vol. 64A, no. 4, July-Aug. 1960, pp. 291-296.
12. Kuo, Chin Y.; and Cheng, Robert Y. K.: Laboratory Requirements for In Situ and Remote Sensing of Suspended Material. NASA CR-145263, 1976.

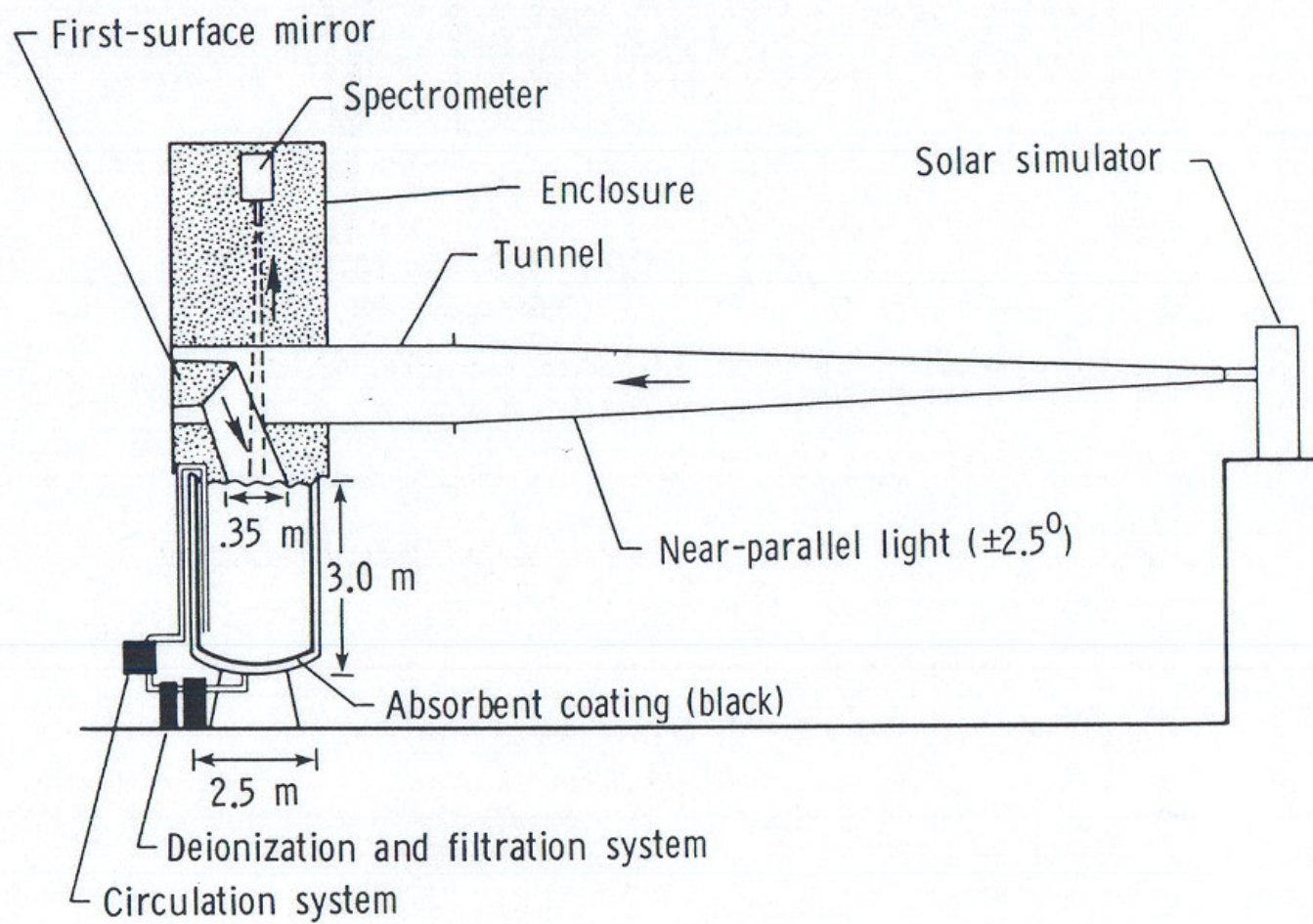
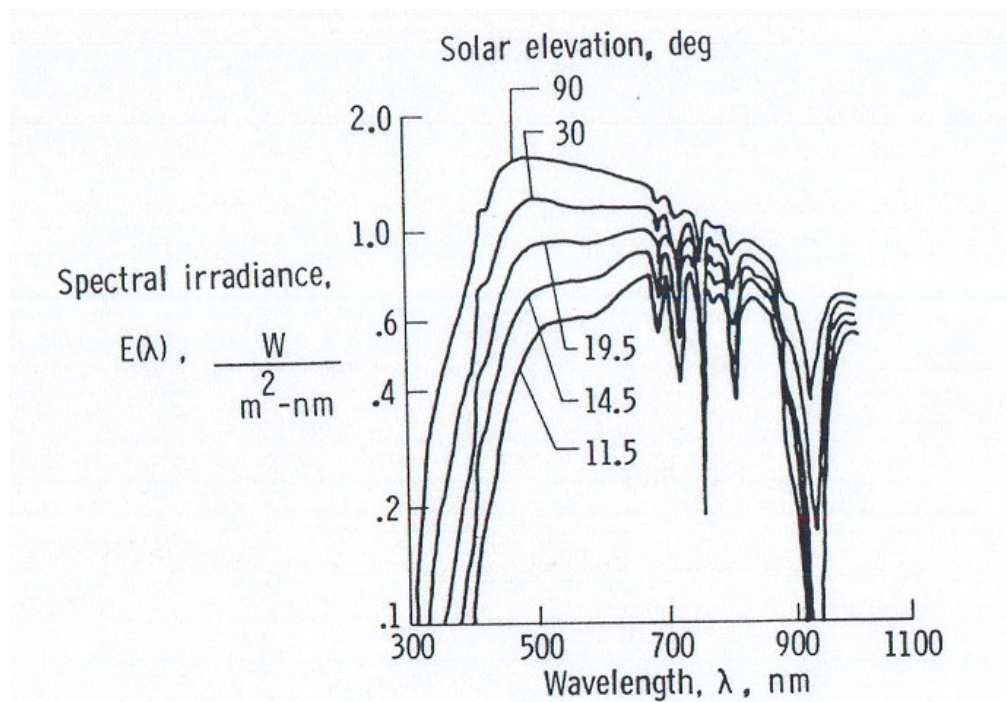
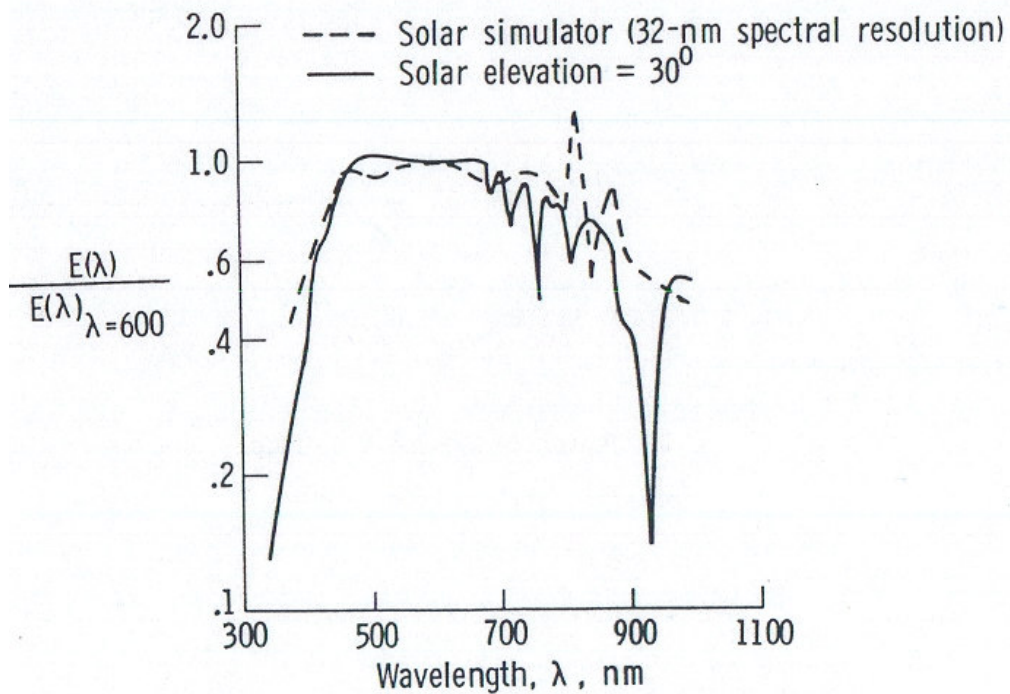


Figure 1.- Sketch of laboratory setup.

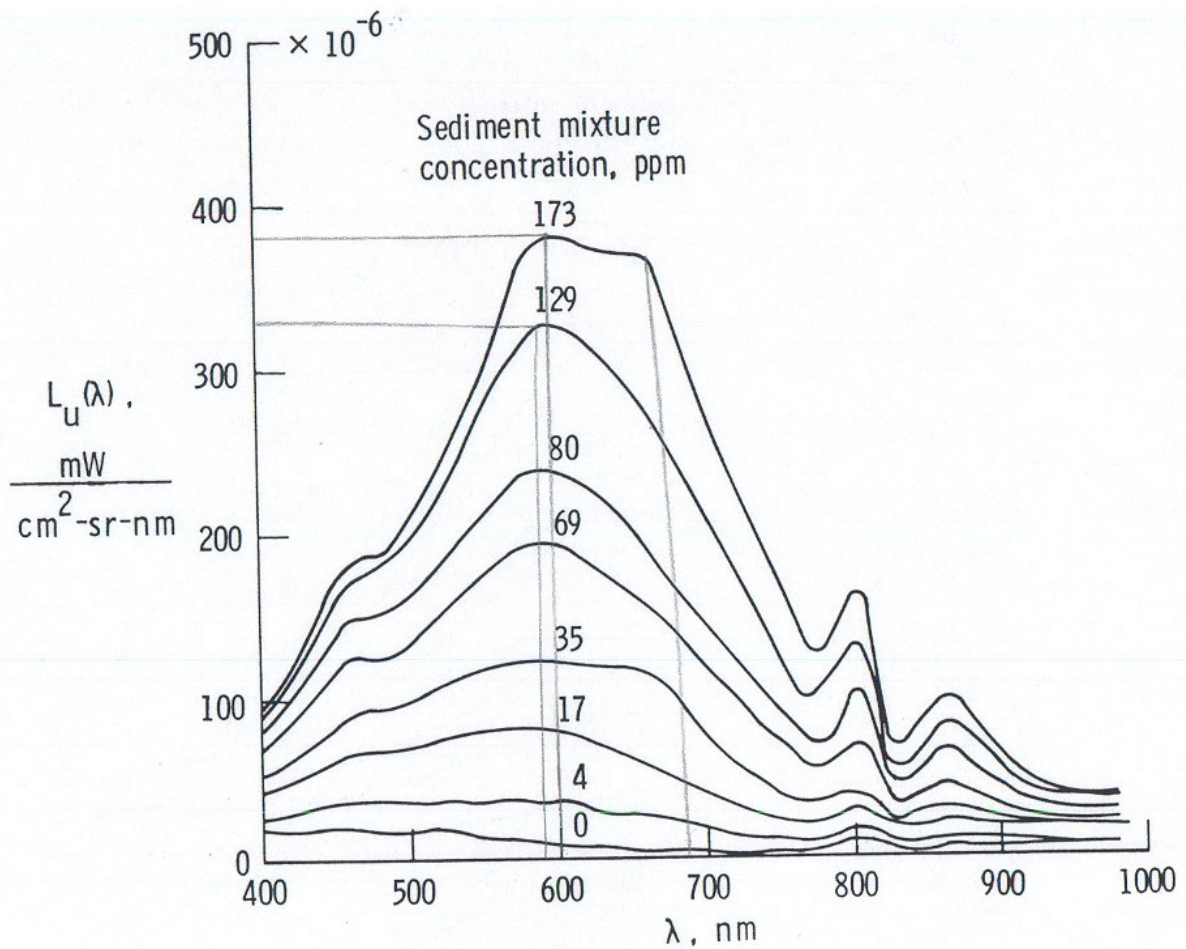


(a) Standard sea-level solar irradiance spectra (ref. 10).



(b) Laboratory and standard sea-level spectra.

Figure 2.- Comparison of laboratory and standard sea-level input spectra.



(a) Spectral resolution of 32 nm.

Figure 3.- Spectral radiance for Calvert soil sediment in filtered, deionized water.

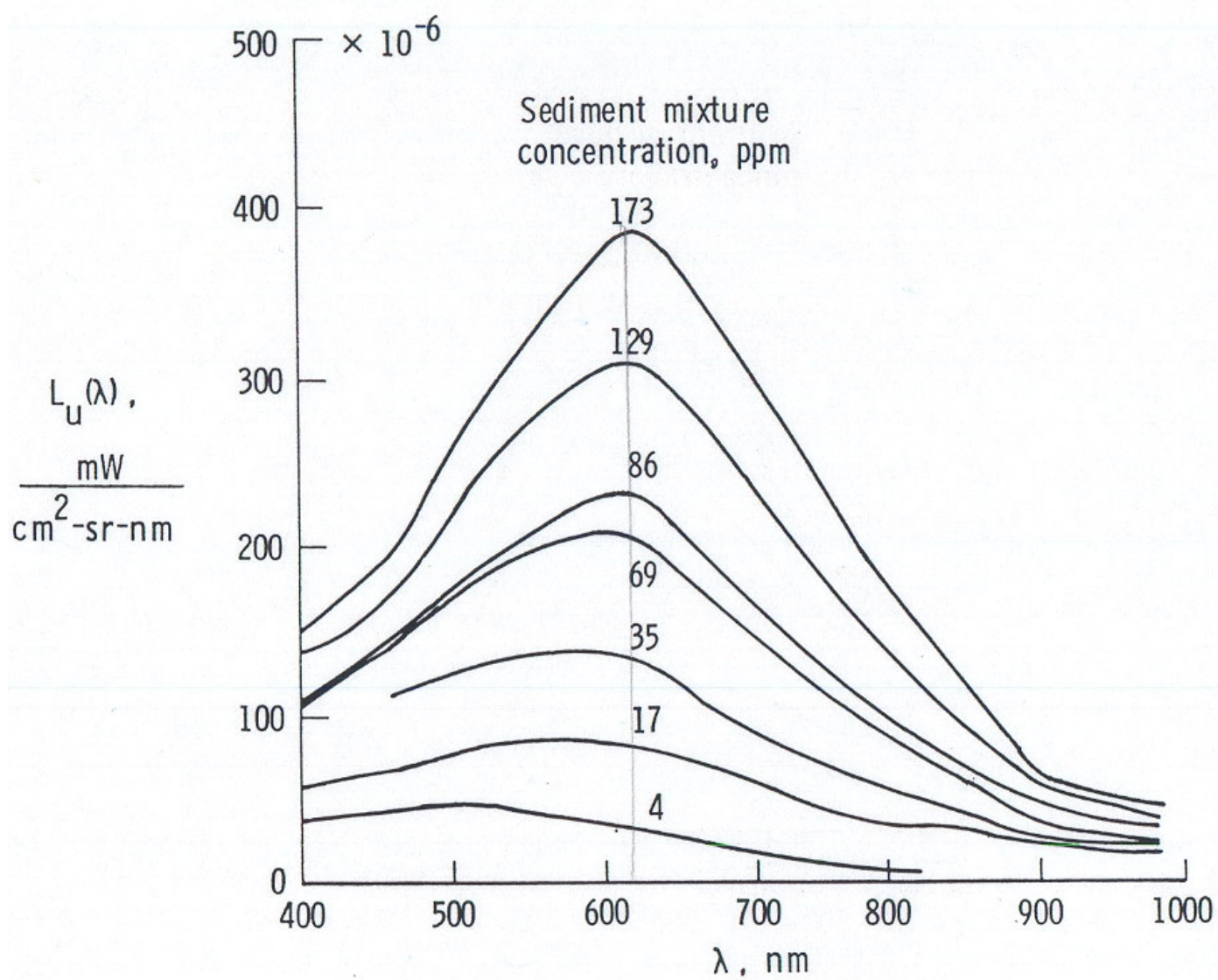
Calvert { higher radiance
peak at $\approx 600 \text{ nm}$
As the concentration increases
the spectra loses the flatness, the
spectral derivative increases -

13

At 4 ppm \rightarrow ratio RED/BLUE ≈ 1

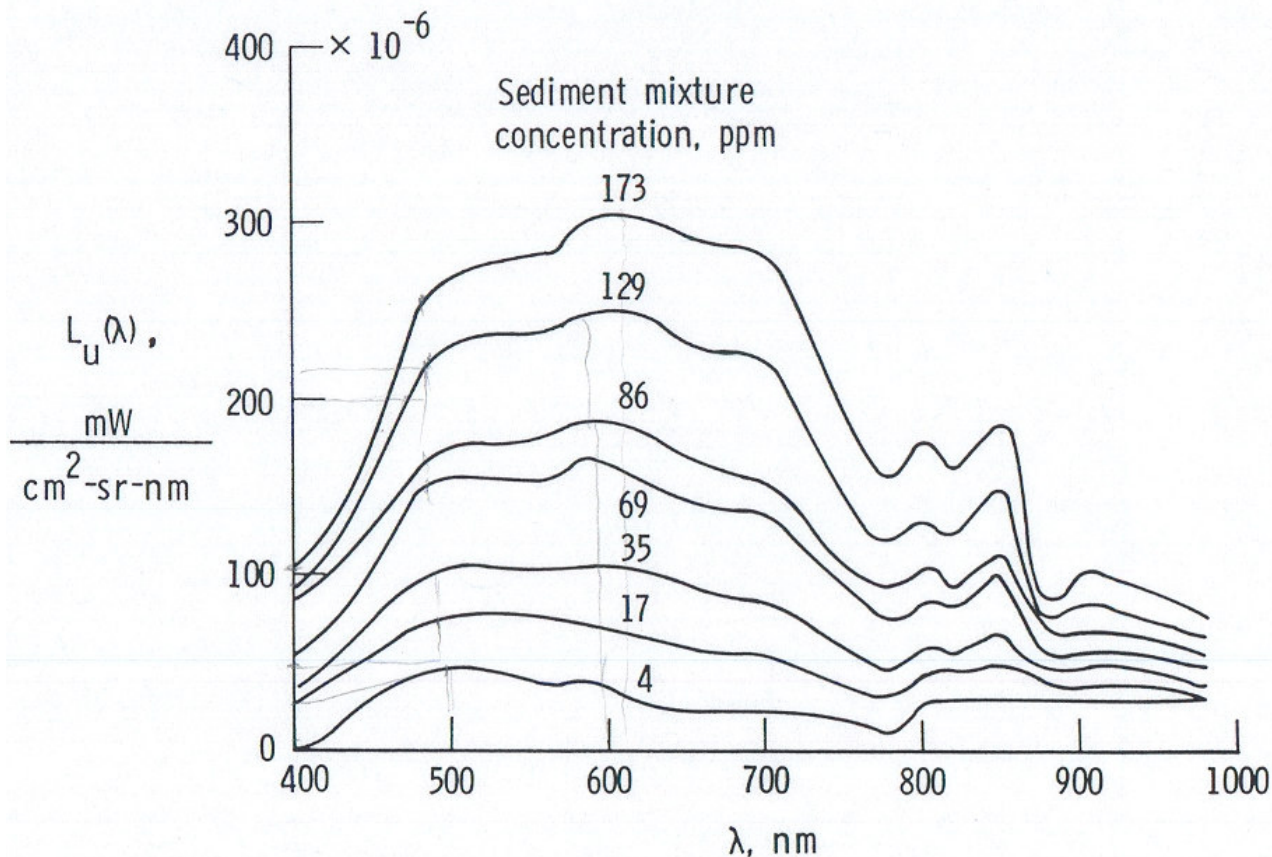
At 129 ppm \rightarrow ratio RED/BLUE ≈ 3

The spectral shape changes with
concentration
and at the saturation \rightarrow it starts
become flatter



(b) Spectral resolution of 160 nm.

Figure 3.- Concluded.



(a) Spectral resolution of 32 nm.

Figure 4.- Spectral radiance for Ball soil sediment in filtered, deionized water.

for 32 nm resolution

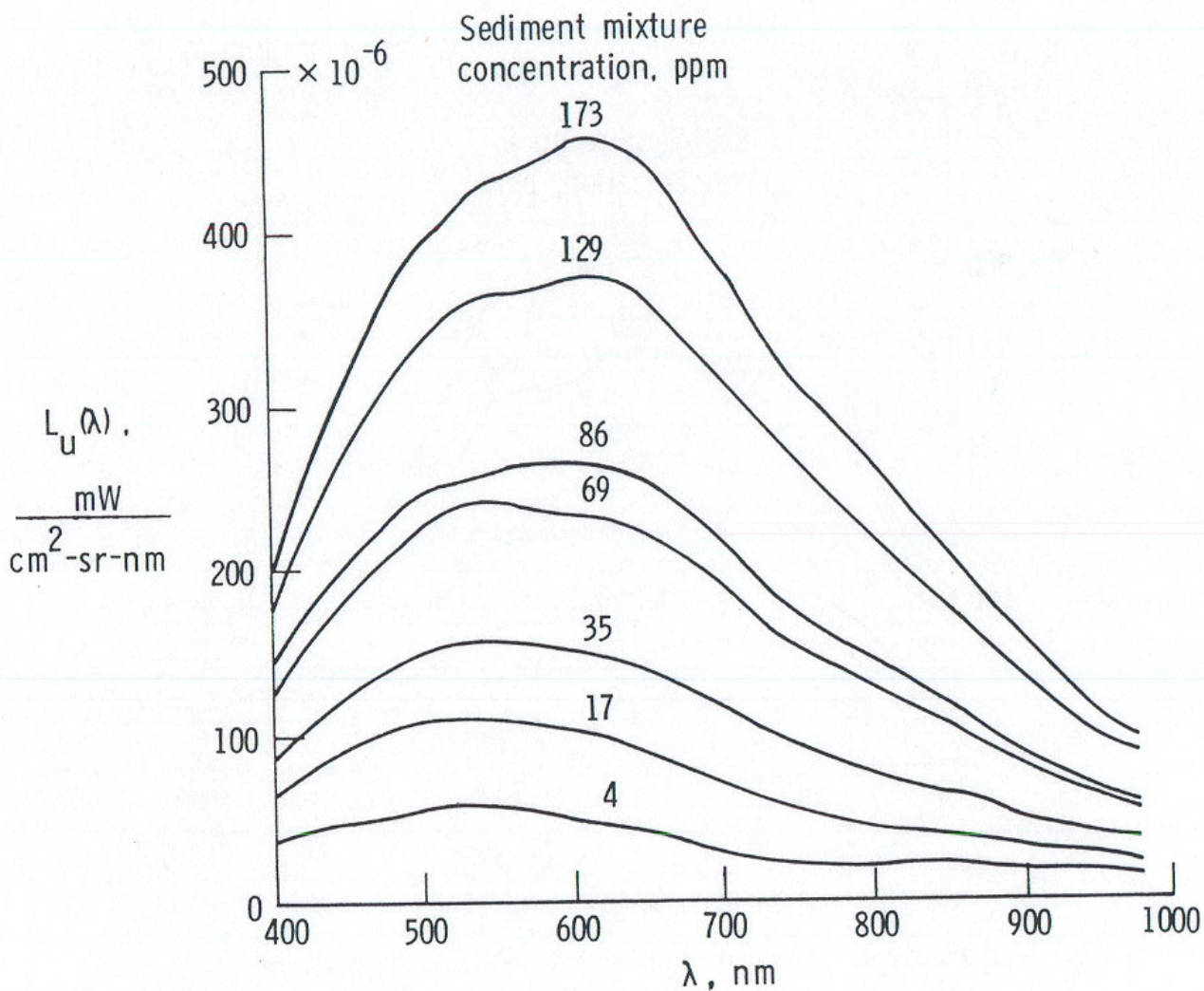
Ball soil →

at 4
Shape is very different from
calvert.

The spectra always have
a plate shape between
500 and 700 nm

15

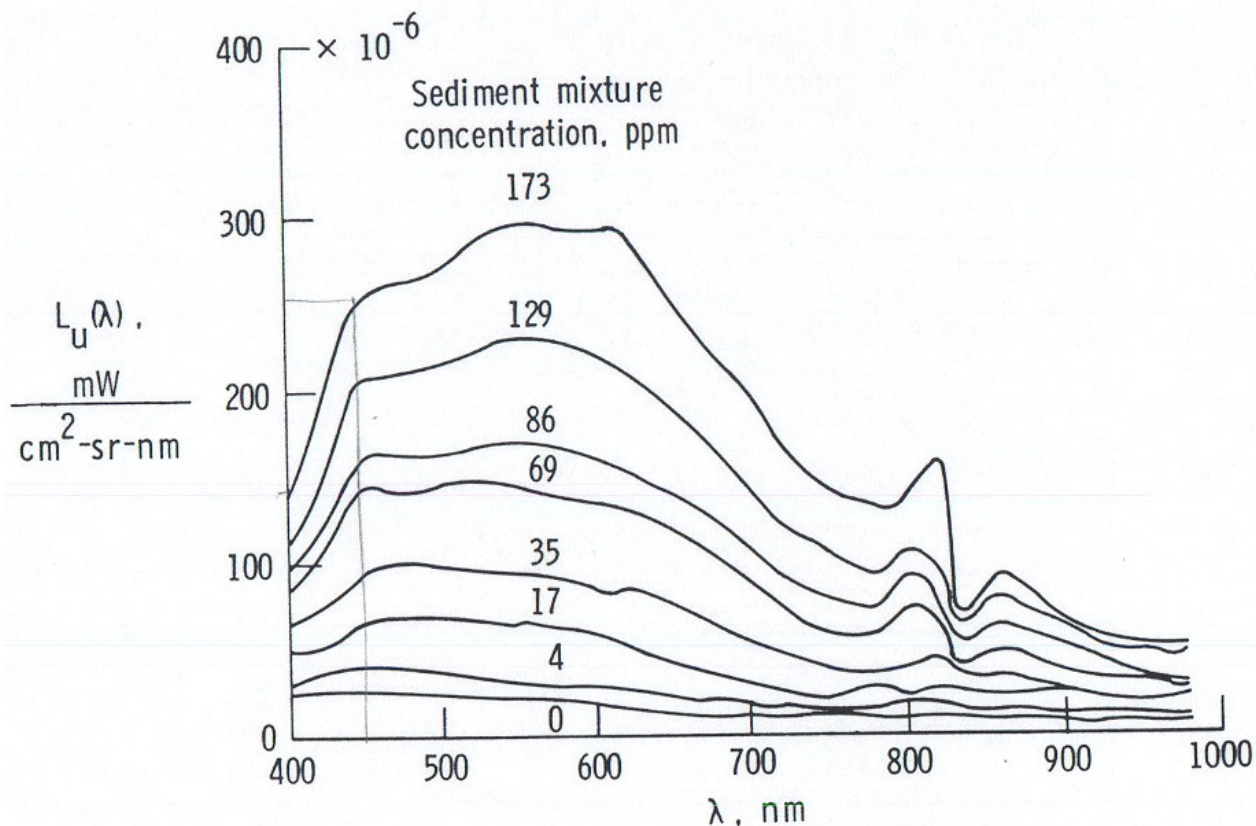
Ratio G/B = 50 at 4 ppm
R G/B
- decreases to 2 at 200 ppm
and then increases to 3
at highest concentration



(b) Spectral resolution of 160 nm.

Figure 4. - Concluded.

→ With lower resolution the "shape" of the spectra is not as distinct from the solvent as for the high resolution. The ratios between blue and green are variable as well.



(a) Spectral resolution of 32 nm.

Figure 5.- Spectral radiance for Jordan soil sediment in filtered, deionized water.

Jordan soil \rightarrow the ratio between 450 and 400 nm would increase with sediment concentration -

0.1 for 4 ppm

1.66 for 173 ppm.

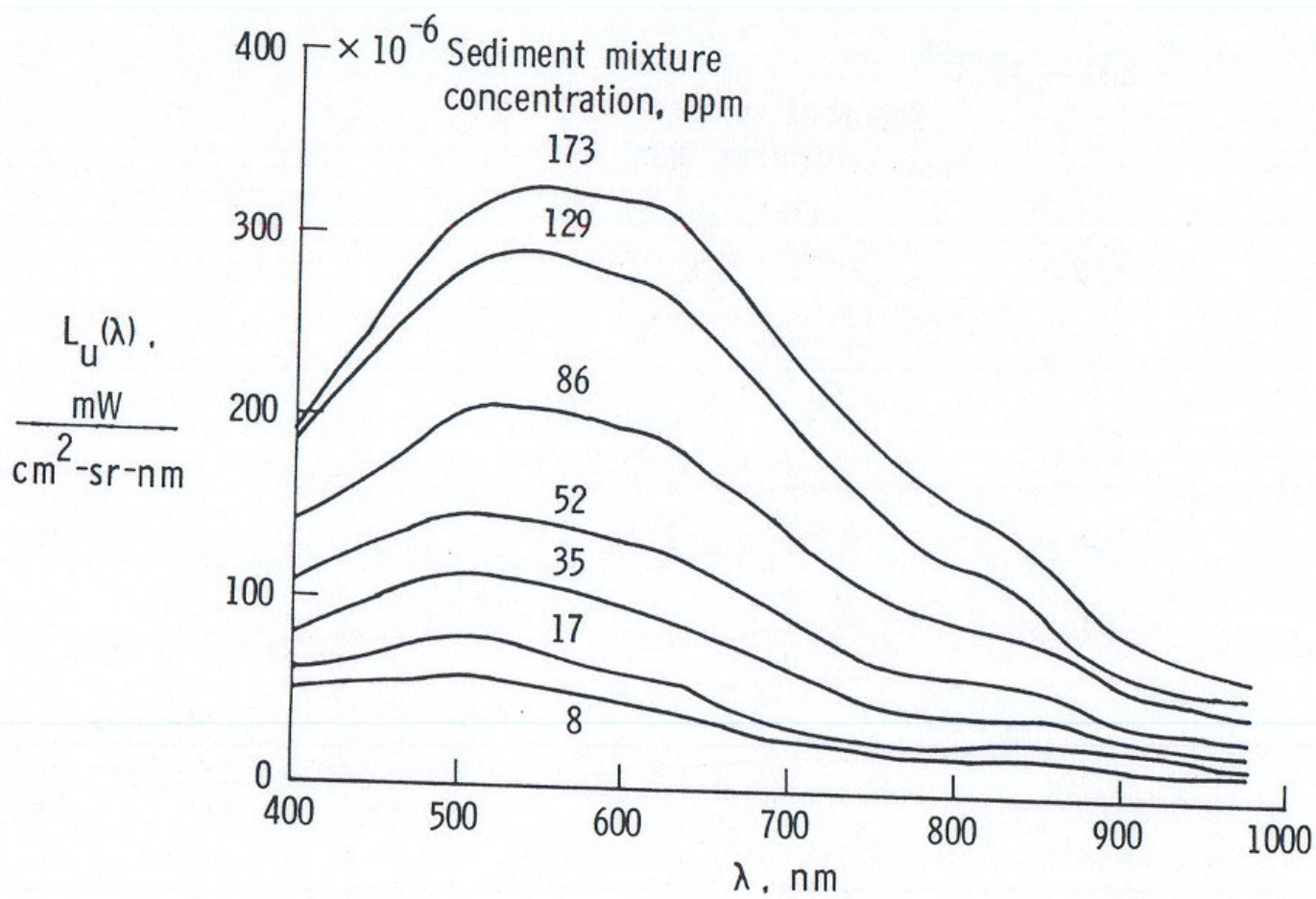
17

up to 86 ppm \Rightarrow reflectance

has a negative gradient

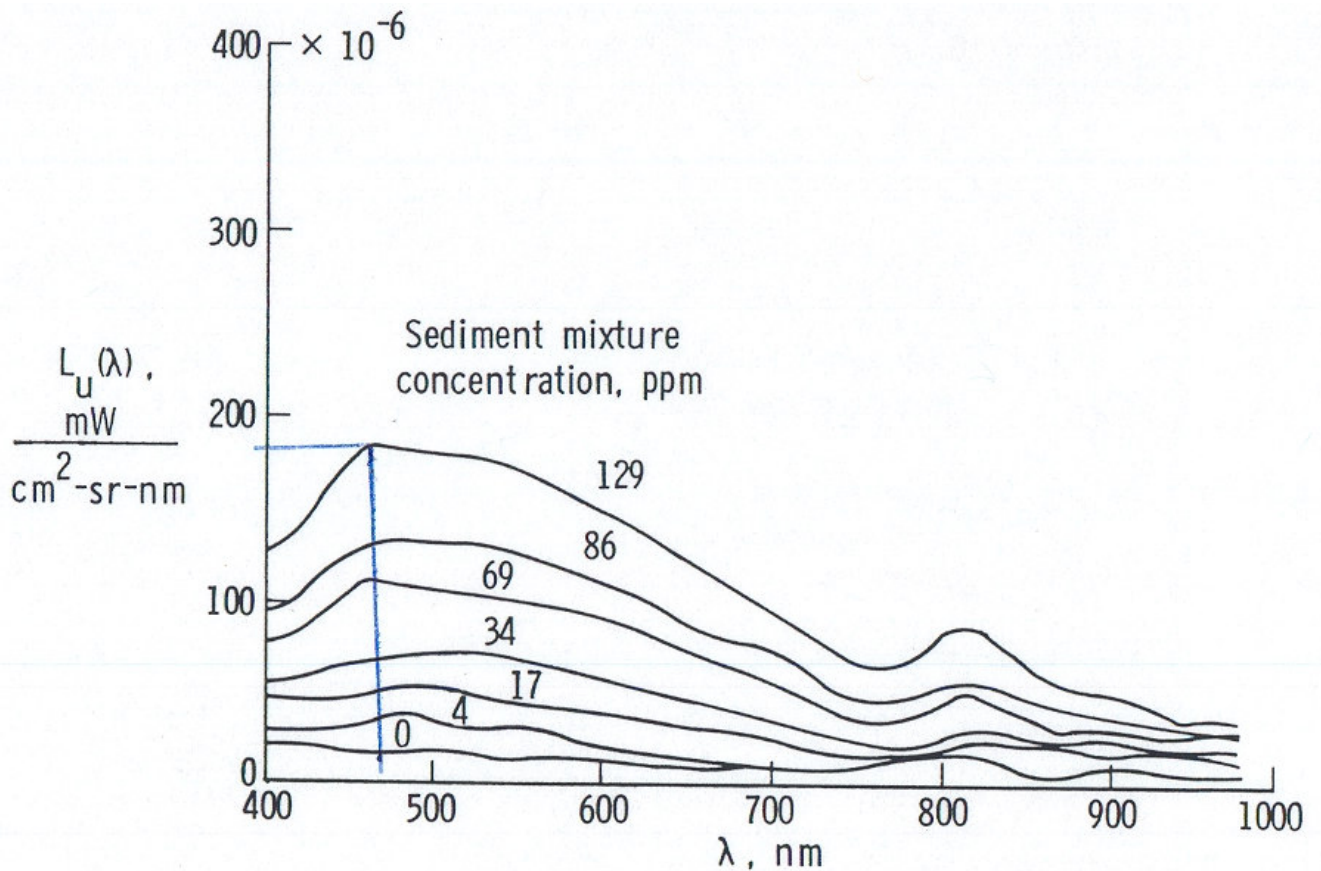
towards the red

from 129 and 173 the gradient is positive.



(b) Spectral resolution of 160 nm.

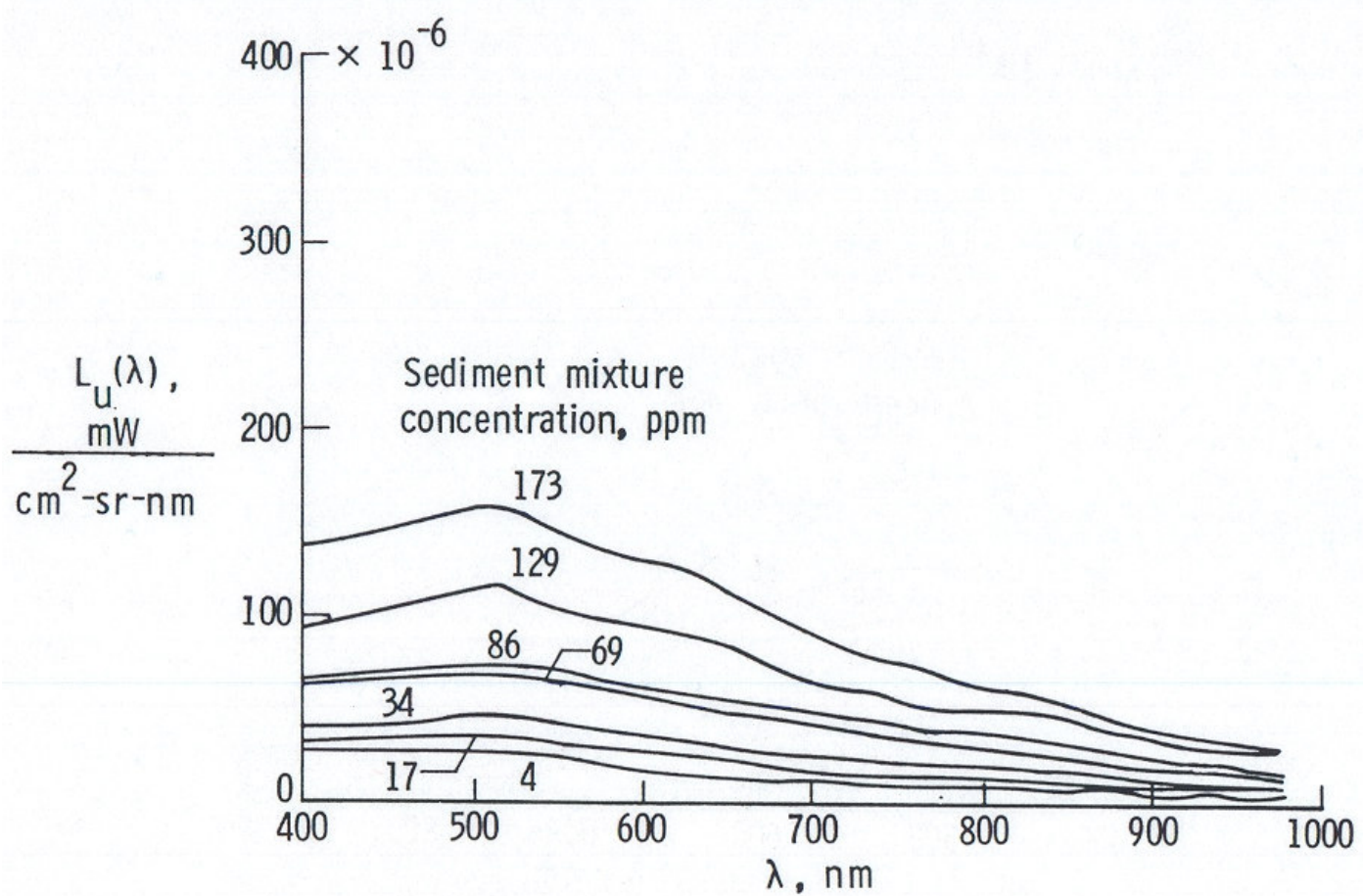
Figure 5.- Concluded.



(a) Spectral resolution of 32 nm.

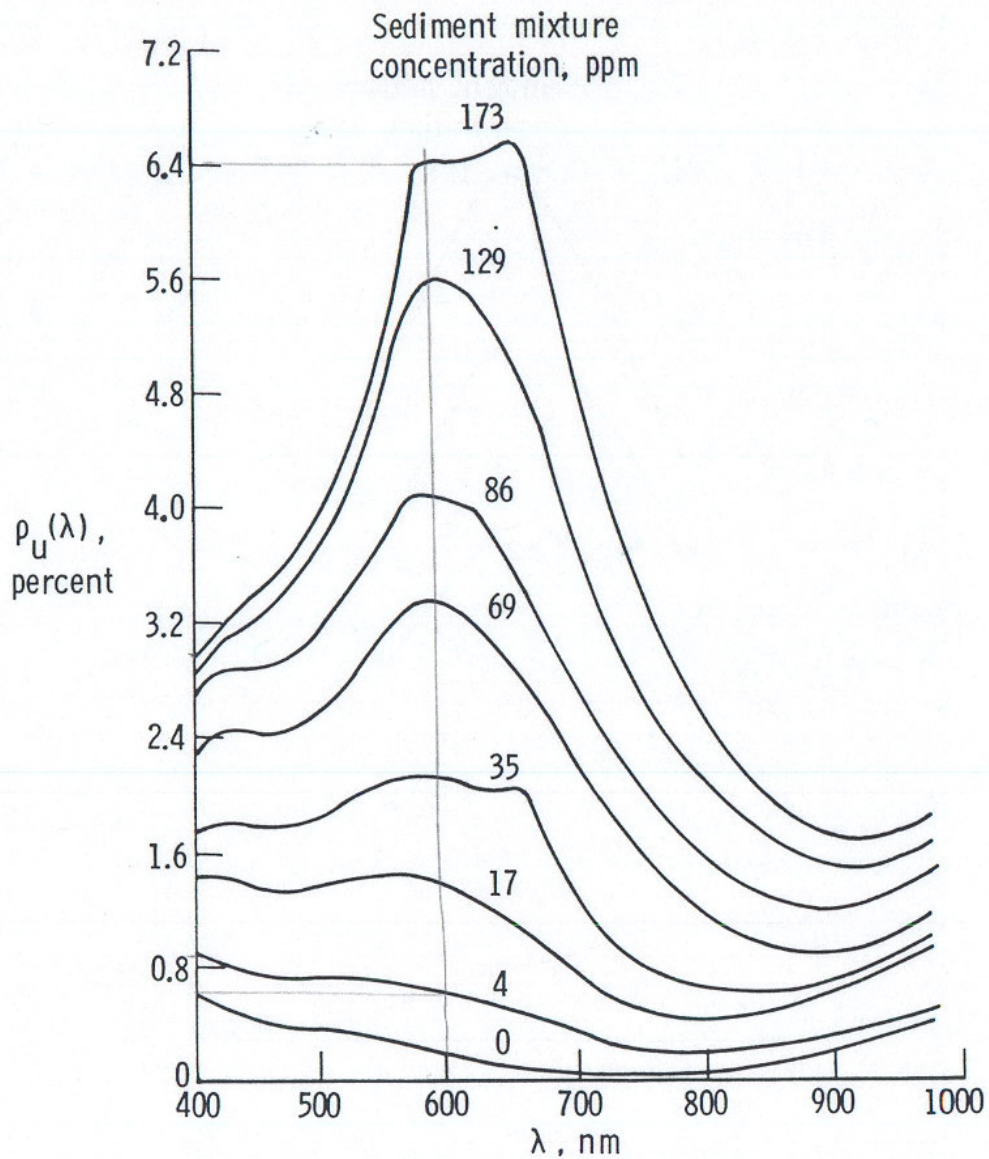
Figure 6.- Spectral radiance for Feldspar soil sediment in filtered, deionized water.

Feldspar \rightarrow lowest radiance
 that spectra up to 3.1 ppm \rightarrow
 type of non-selective
 scattering



(b) Spectral resolution of 160 nm.

Figure 6. - Concluded.



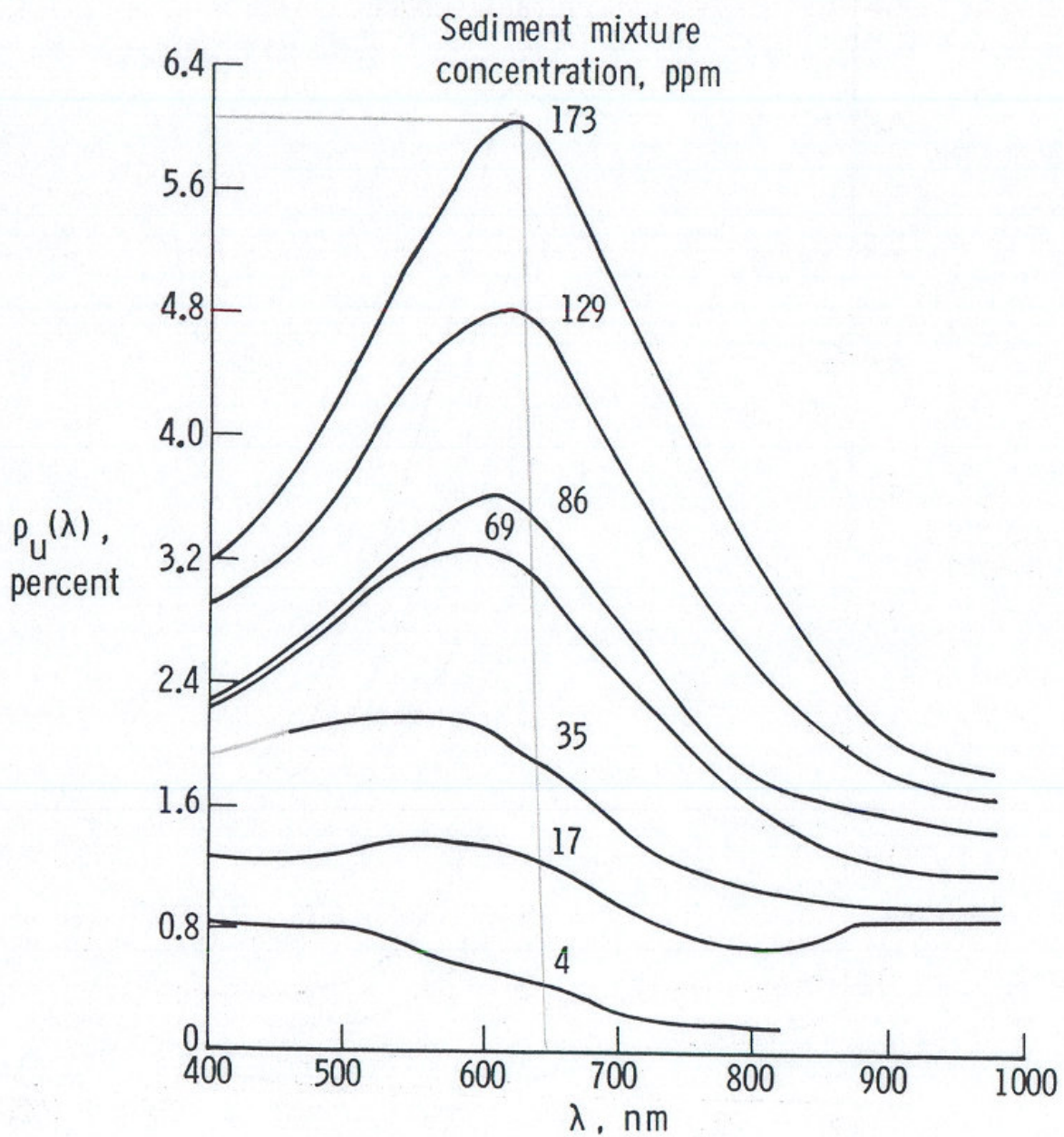
(a) Spectral resolution of 32 nm.

Figure 7.- Spectral reflectance for Calvert soil sediment in filtered, deionized water.

$$\text{Calvert} = \rho_{600}/\rho_{400} \approx \begin{matrix} 2.4 \rightarrow 173 \text{ ppm} \\ 0.7 \rightarrow 4 \text{ ppm} \end{matrix}$$

17 ppm \rightarrow spectra is ²¹
flat through
blue/green wavelength

maximum reflect. at 700 nm = 6.4%



(b) Spectral resolution of 160 nm.

Figure 7.- Concluded.

maximum reflectance is
at 650nm and
6%
fail to detect

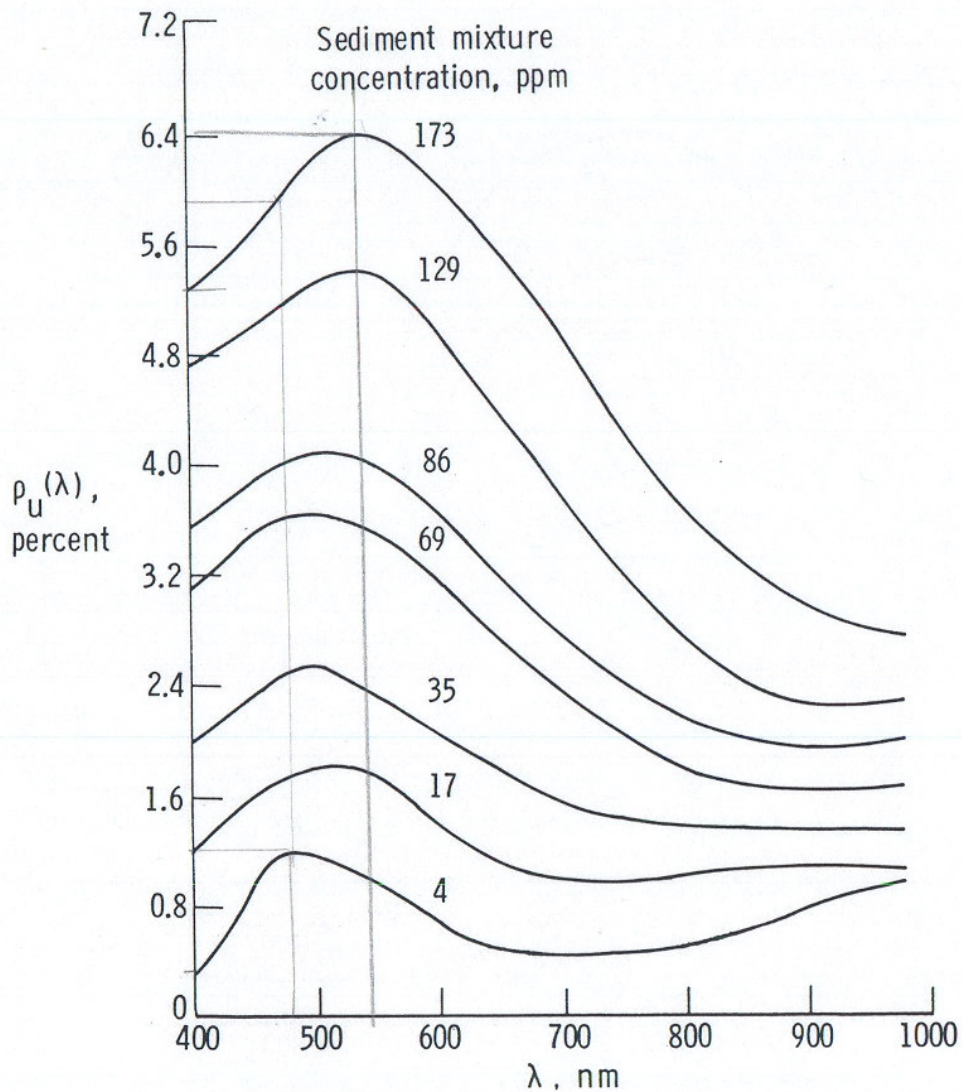


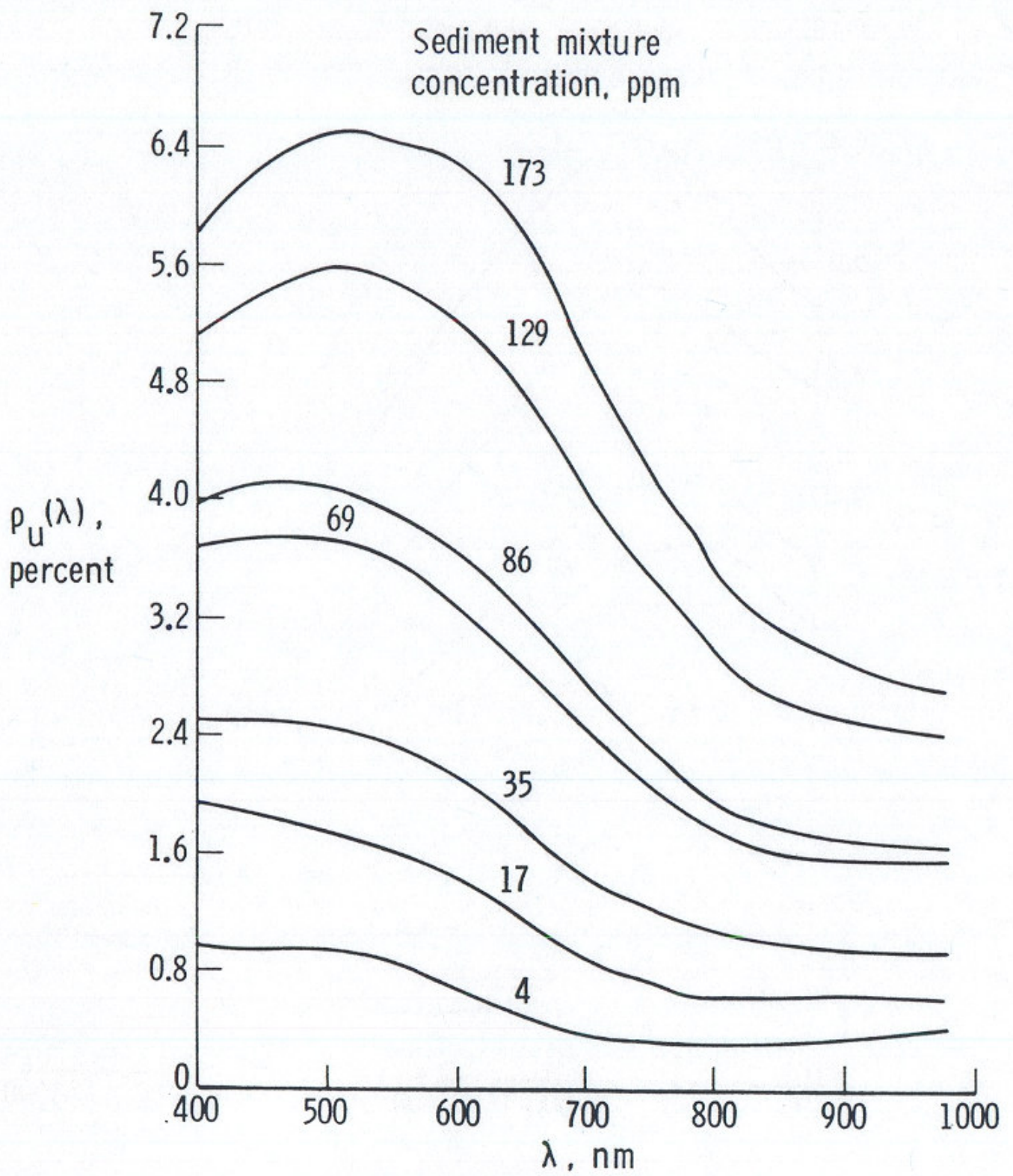
Figure 8.- Spectral reflectance for Ball soil sediment in
filtered, deionized water.

Ball \rightarrow does not have the
plateau between
600 and 700 nm

23

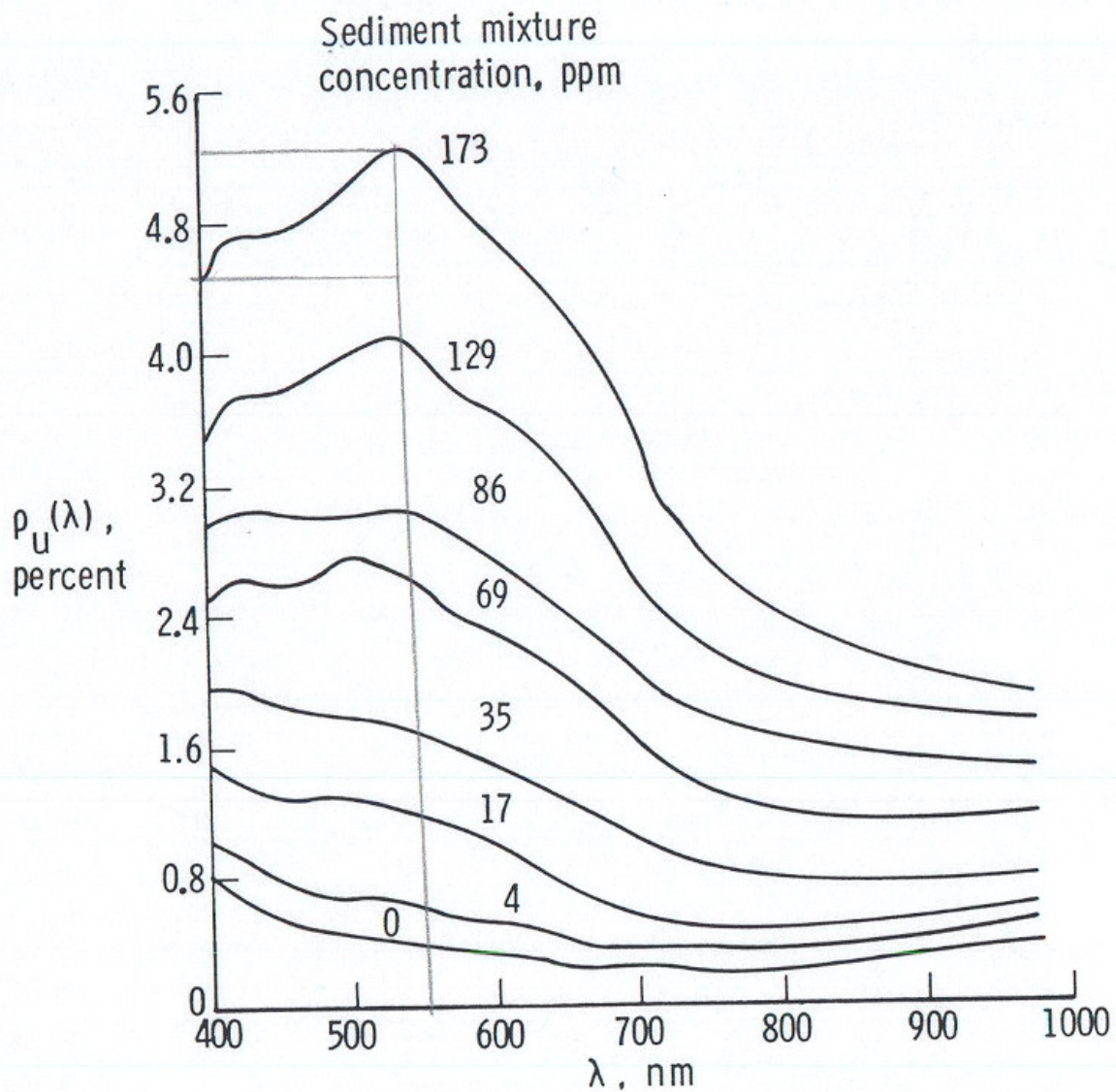
it has the a higher ratio
between 480/400 at
4 ppm ≈ 3.00

Ratio 650/400 ≈ 1.2 for
concentration ≥ 129 ppm



(b) Spectral resolution of 160 nm.

Figure 8.- Concluded.

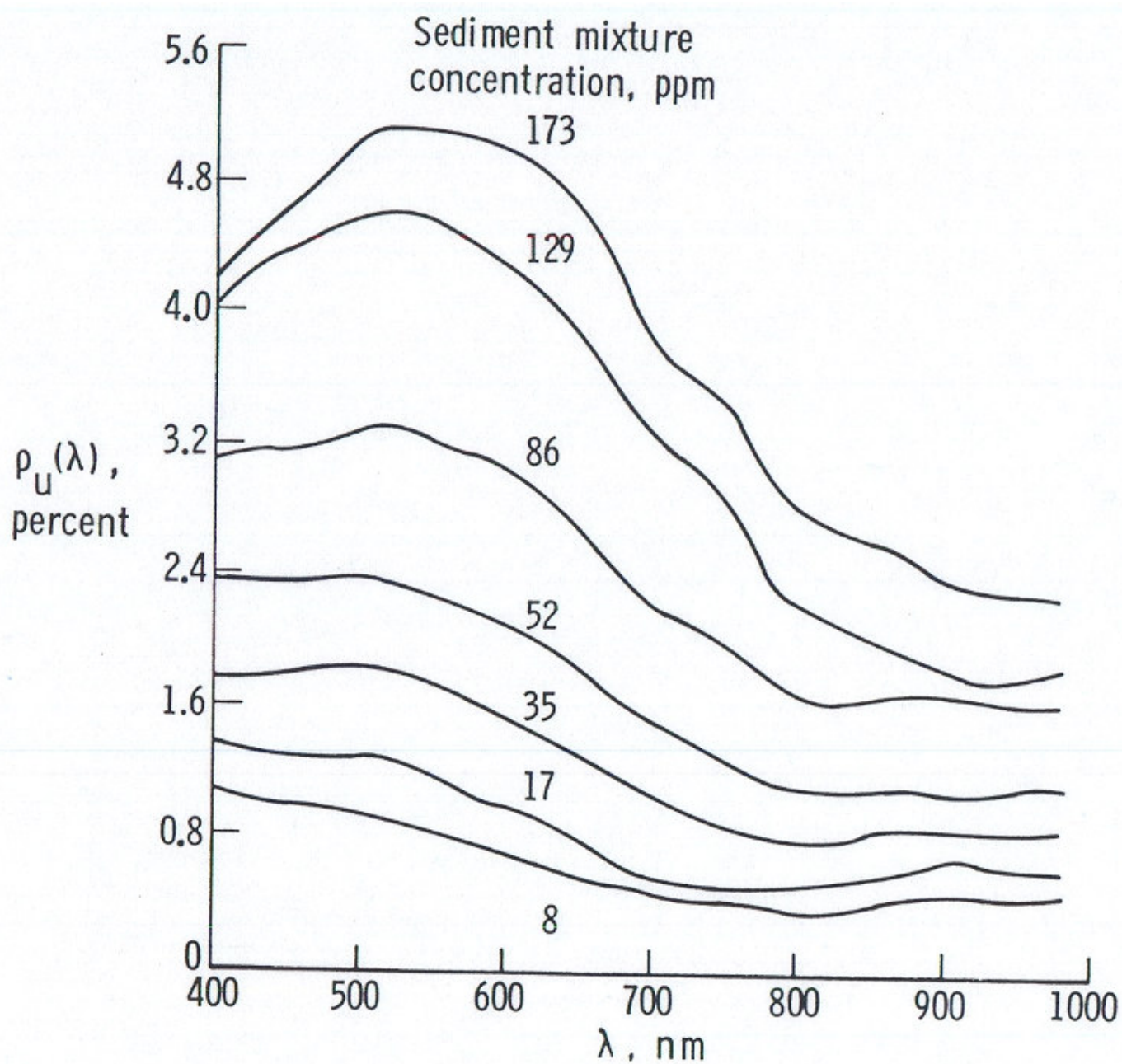


(a) Spectral resolution of 32 nm.

Figure 9.- Spectral reflectance for Jordan soil sediment in filtered, deionized water.

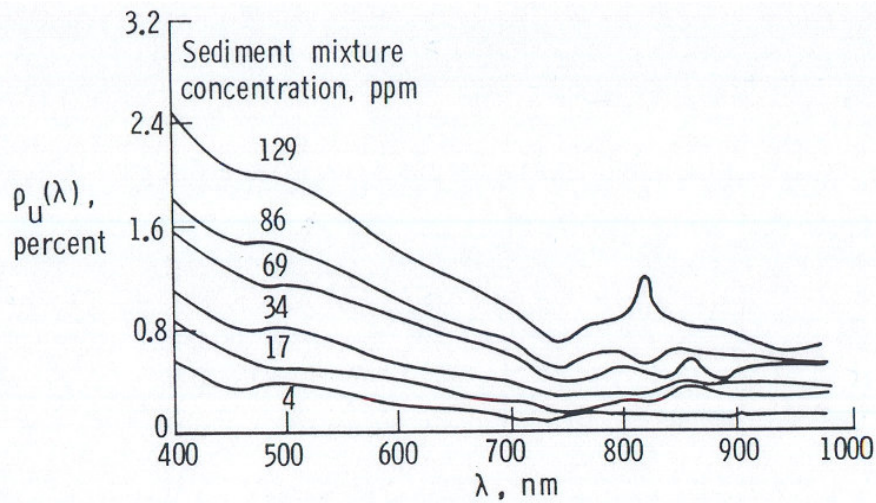
Jordan Soil - ratio $550/400 \approx 0.80$
for 4 ppm

Jordan Soil - ratio $550/400 \approx 1.20$
for 173 ppm

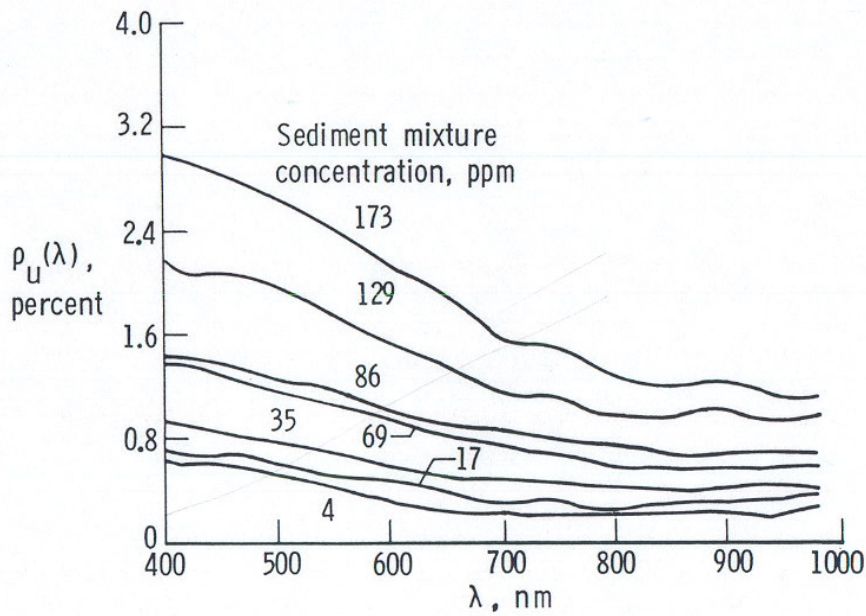


(b) Spectral resolution of 160 nm.

Figure 9.- Concluded.



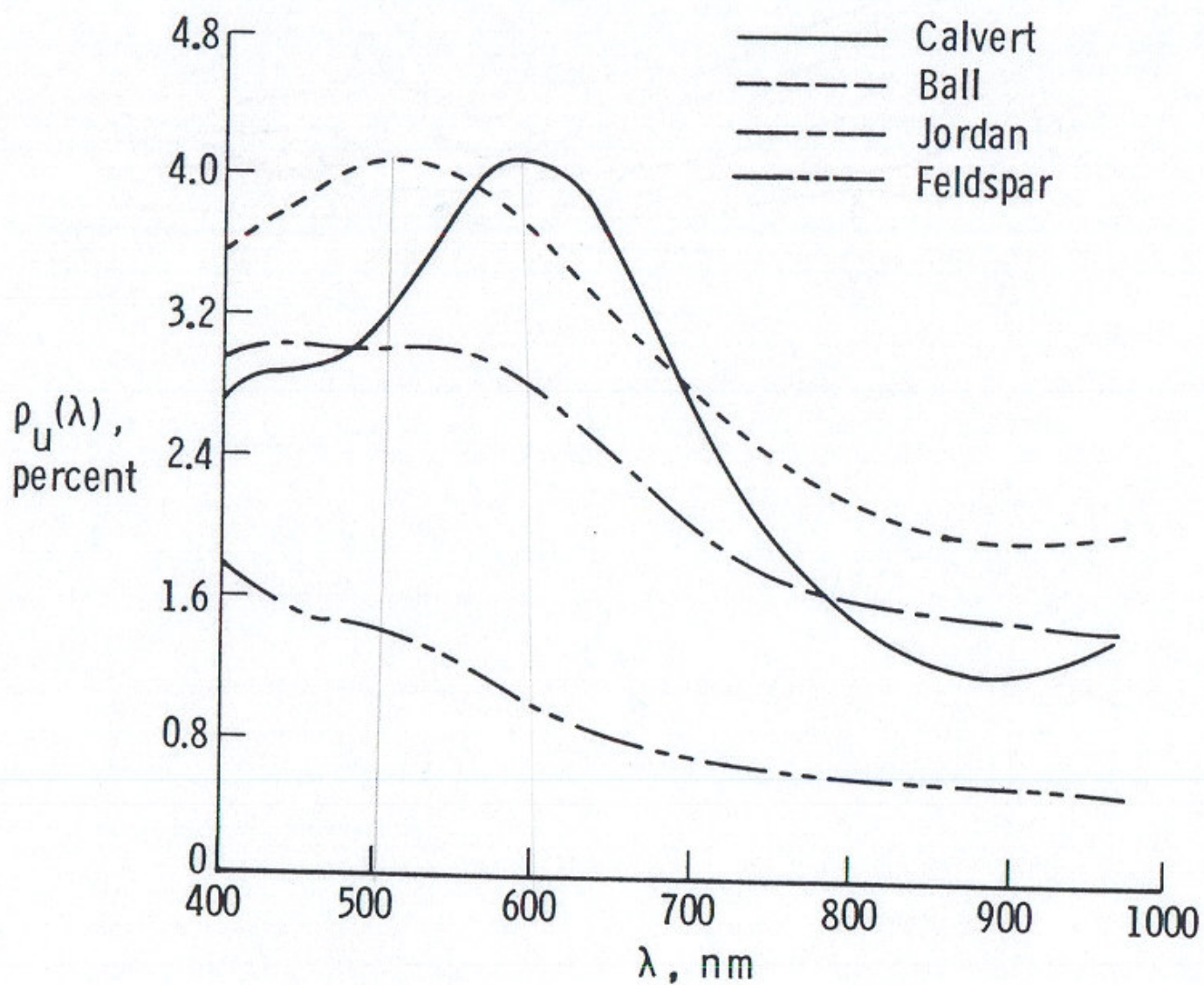
(a) Spectral resolution of 32 nm.



(b) Spectral resolution of 160 nm.

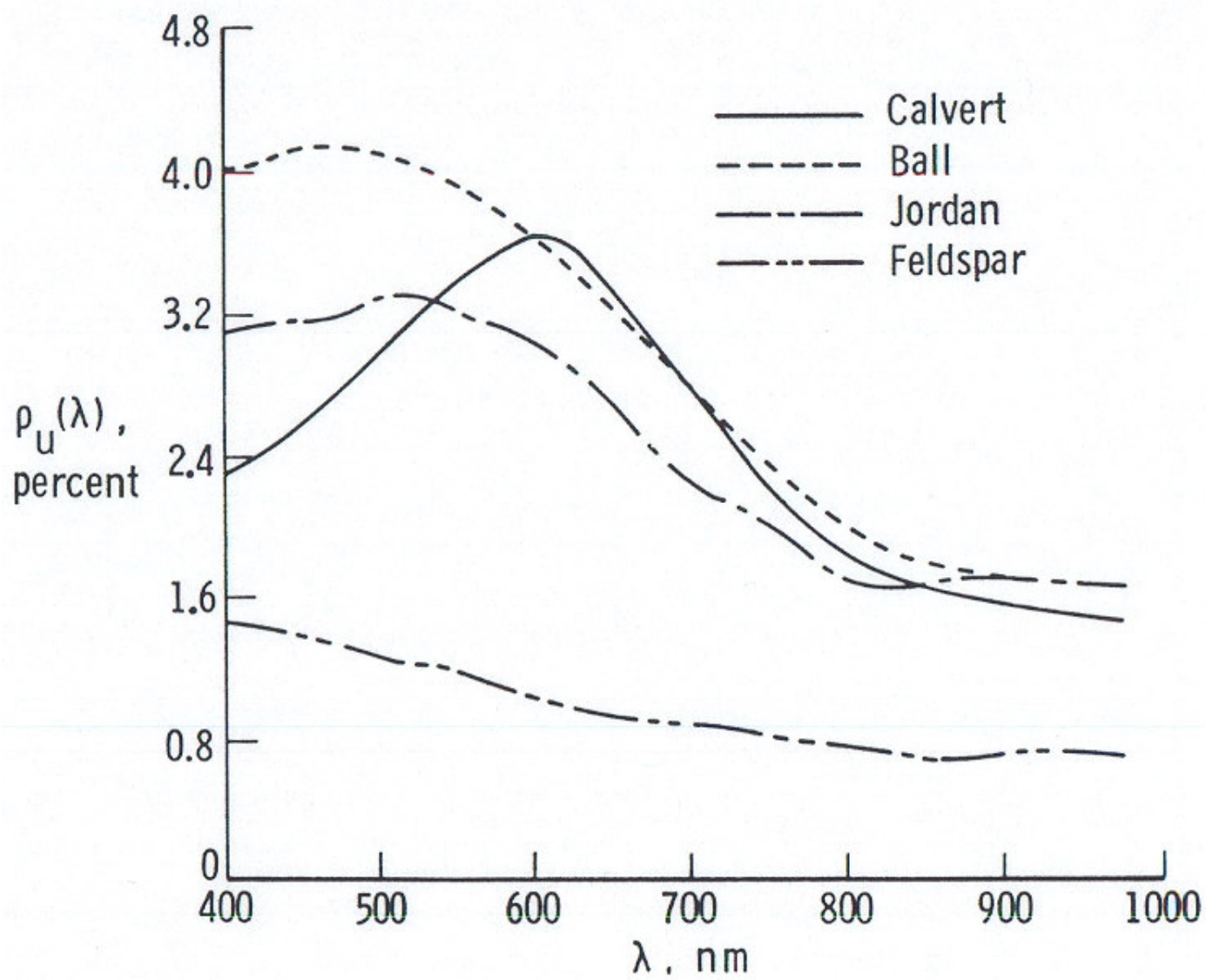
Figure 10.- Spectral reflectance for Feldspar soil sediment in filtered, deionized water.

27
Feldspar = decreasing gradient - 8
Just increases the water reflectance but actually does not change the shape



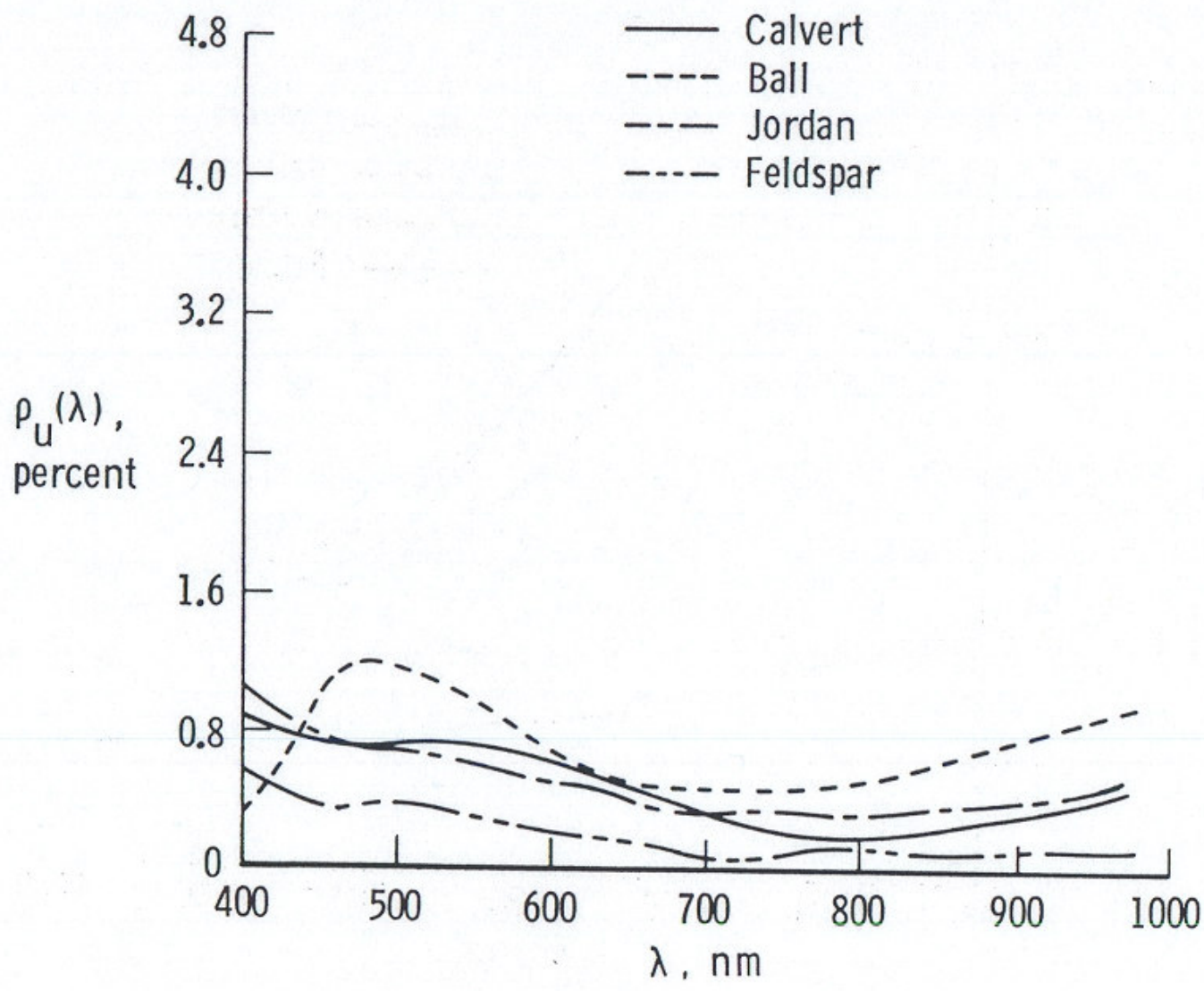
(a) Spectral resolution of 32 nm.

Figure 11.- Comparison of spectral reflectance for four sediments at mixture concentration of 86 ppm.



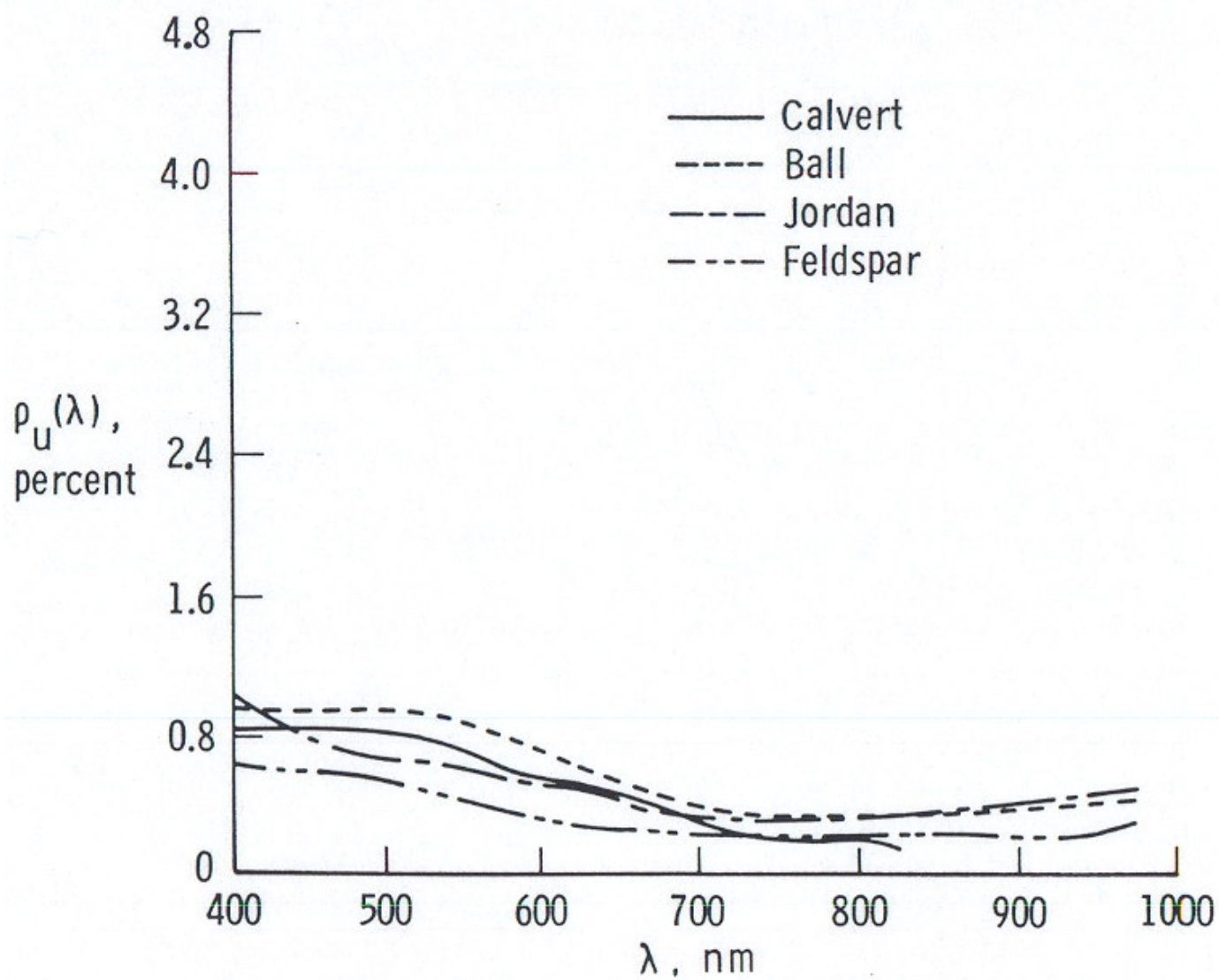
(b) Spectral resolution of 160 nm.

Figure 11.- Concluded.



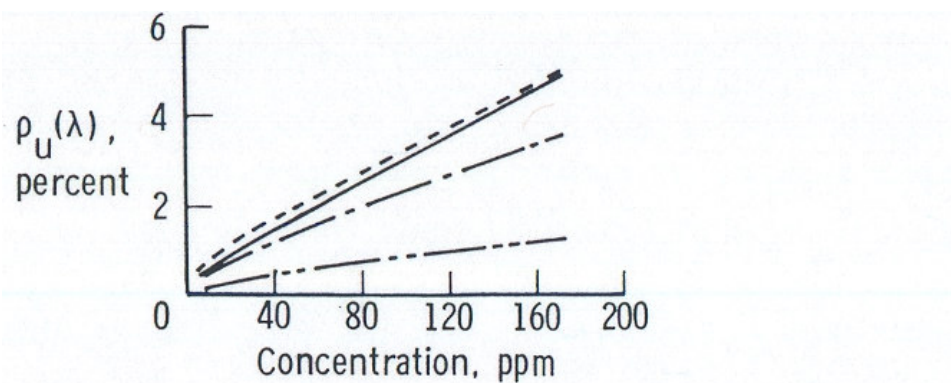
(a) Spectral resolution of 32 nm.

Figure 12.- Comparison of spectral reflectance for four sediments at mixture concentration of 4 ppm.

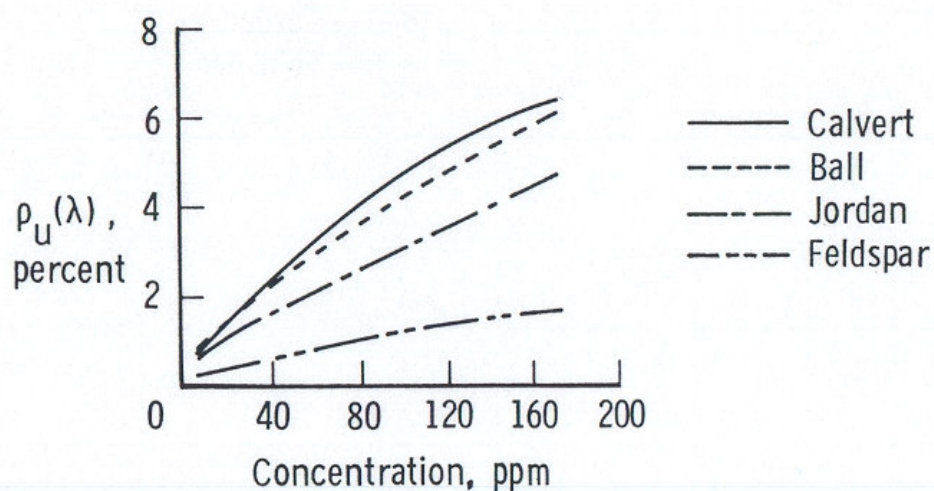


(b) Spectral resolution of 160 nm.

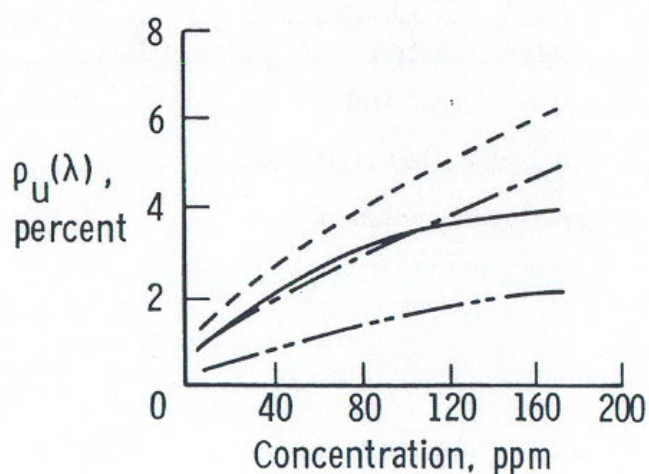
Figure 12.- Concluded.



(a) $\lambda = 700$ nm.



(b) $\lambda = 600$ nm.



(c) $\lambda = 500$ nm.

Figure 13.- Variation of spectral reflectance with concentration.
Spectral resolution of 32 nm.

| | | | | | |
|--|--|-----------------------------|----------------------|---|--|
| 1. Report No. NASA TP-1039 | | 2. Government Accession No. | | 3. Recipient's Catalog No. | |
| 4. Title and Subtitle LABORATORY MEASUREMENTS OF UPWELLED RADIANCE AND REFLECTANCE SPECTRA OF CALVERT, BALL, JORDAN, AND FELDSPAR SOIL SEDIMENTS | | | | 5. Report Date December 1977 | |
| | | | | 6. Performing Organization Code | |
| 7. Author(s) Charles H. Whitlock, J. W. Usry, William G. Witte, and E. A. Gurganus | | | | 8. Performing Organization Report No. L-11854 | |
| 9. Performing Organization Name and Address NASA Langley Research Center Hampton, VA 23665 | | | | 10. Work Unit No. 177-55-31-01 | |
| | | | | 11. Contract or Grant No. | |
| | | | | 13. Type of Report and Period Covered Technical Paper | |
| 12. Sponsoring Agency Name and Address National Aeronautics and Space Administration Washington, DC 20546 | | | | 14. Sponsoring Agency Code | |
| | | | | | |
| 15. Supplementary Notes | | | | | |
| 16. Abstract <p>A limited effort to investigate the potential of remote sensing for monitoring nonpoint source pollution was conducted. Spectral reflectance characteristics for four types of soil sediments were measured for mixture concentrations between 4 and 173 ppm. For measurements at a spectral resolution of 32 nm, the spectral reflectances of Calvert, Ball, Jordan, and Feldspar soil sediments were distinctly different over the wavelength range from 400 to 980 nm at each concentration tested. At high concentrations, spectral differences between the various sediments could be detected by measurements with a spectral resolution of 160 nm. At a low concentration (4 ppm), only small differences were observed between the various sediments when measurements were made with 160-nm spectral resolution. Radiance levels generally varied in a nonlinear manner with sediment concentration; linearity occurred in special cases, depending on sediment type, concentration range, and wavelength.</p> | | | | | |
| 17. Key Words (Suggested by Author(s)) Remote sensing Spectral signature Laboratory measurements Environmental monitoring Marine sediments | | | | 18. Distribution Statement Unclassified - Unlimited Subject Category 48 | |
| 19. Security Classif. (of this report) Unclassified | 20. Security Classif. (of this page) Unclassified | 21. No. of Pages 32 | 22. Price* \$4.50 | | |

* For sale by the National Technical Information Service, Springfield, Virginia 22161

NASA-Langley, 1977